RECENT DEVELOPMENTS IN ATCOR FOR ATMOSPHERIC COMPENSATION AND RADIOMETRIC PROCESSING OF IMAGING SPECTROSCOPY DATA

Daniel Schläpfer[1]*, and Rudolf Richter*[2]

1. ReSe Applications, Wil SG, Switzerland; Daniel(at)rese.ch
2. German Aerospace Center (DLR), Weßling, Germany; rudolf.richter(at)dlr.de

ABSTRACT

Recent developments in atmospheric compensation are summarized in this paper with emphasis on algorithms implemented in the ATCOR model. First, achievements and current limitations in haze and aerosol detection and correction as well as in *BRDF* correction are outlined. Secondly, correction approaches for high resolution spectral variations in the reflectance outputs are described. The inherent problem of high resolution imaging spectroscopy is that smallest spectral variations of the instrument response during data acquisition, radiative transfer model errors in atmospheric gas absorption, and errors in the employed solar irradiance spectrum lead to significant spectral variations after atmospheric compensation. Applying spectral recalibration and using air pressure dependent processing is shown to improve the comparability of the radiometrically corrected reflectance data to the ground measurements and to modelled spectra. Remaining open issues are the aerosol scattering compensation below 420 nm wavelength, the model-based *BRDF* correction in rugged terrain, and the correct consideration of spectral band width during processing.

KEYWORDS

Atmospheric correction, radiometric compensation, ATCOR, BRDF, BREFCOR, spectral calibration, radiative transfer model

INTRODUCTION

The goal of atmospheric compensation of imaging spectroscopy is to provide accurate measurements of surface reflectance information. Spectral analysis in comparison to singular library spectra such as target detection or spectral unmixing methods as well as spectral indices is usually applied without consideration of the observation angle. For such analyses, the bi-hemispherical reflectance (i.e., the spectral albedo, blue-sky albedo *BHR* (1)) would be the quantity of interest as it is the only reflectance quantity unbiased by illumination and observation angles. On the other hand, if the data is to be analysed by model inversion, the directionality of the observation is to be considered. In these cases, the hemispherical-directional reflectance (*HDRF*) (1) is the preferred quantity for data analyses.

The methods to determine these quantities from the at-sensor radiance measurements have been in development for more than 30 years (2,3,4). The processing methods have undergone substantial improvements recently and many operationally usable methods and changes have been gradually included in the ATCOR® software package (5). Currently, a transition is ongoing from standard atmospheric correction using empirical assumptions to an integral, fully automatic and model-based radiometric processing. The related developments in the ATCOR atmospheric compensation model are outlined in this paper.

Pure radiometric modelling and processing rely on high quality data calibration (6), a topic which is not covered by this paper even though it is considered a crucial precondition. The atmospheric compensation part requires knowledge about the state of the atmosphere. Recently, substantial

DOI: 10.12760/02-2015-2-04

progress has been made in haze detection and correction (7) as well as in the understanding of spectral signatures at low irradiance conditions and in the blue wavelength range. The resulting improved haze correction methods and related observations for the correction of aerosol scattering signatures are summarized hereafter.

A second topic which has been addressed recently is the retrieval of *BHR* values by correction of *BRDF* influences on the data. The bi-directional effects are to be corrected on both the incident direction and the observer side. The incidence *BRDF* correction shows its advantages specifically in rugged terrain (8), whereas the observer *BRDF* correction improves the consistency of wide *FOV* instruments. The recently established BREFCOR method (9) is shortly described and the observed effects are shown hereafter.

With the availability of very high spectral resolution airborne instruments, another focus has been put on the optimization of the spectral accuracy. In the past years, some efforts have been made to find the optimal representation of the solar spectrum and it was decided to use the recent solar irradiance spectrum of Fontenla (10) as a standard reference. Further, the correction with consideration of the spectral smile of a system has been added to the ATCOR model (11). Nevertheless, the spectral accuracy of atmospheric compensation needs further improvement (12). Some recent adjustments with respect to the air pressure dependency are shown herein.

HAZE AND AEROSOL CORRECTION

An improved de-hazing method has been developed (7). The algorithm removes spatially varying haze based on a haze thickness map (HTM). It is calculated by statistical analysis of dark objects within the imagery, using a moving window technique. Bright object areas, which might be misclassified as haze, are excluded from the HTM map. These areas are spatially interpolated in the second processing step. Generally, haze reduces the atmospheric transmittance and adds an additional path radiance to the total radiance at the sensor. However, we use a simplified model, where only the additive component is treated, i.e.: $L_{at-sensor} = L_{scene} + L_{haze}$. This component is subtracted before applying the standard atmospheric compensation.

As demonstrated in Figure 1 and the scenes presented in (7), even the simplified method achieves a distinct improvement when compared to the original hazy scene. For a detailed description of the method the interested reader has to be referred to (7).

Figure 1: Haze correction sample result on Worldview-2 data.

Compared to the former haze algorithm, which is applicable in the blue-NIR region, the new method treats all bands from the blue to the short-wave spectral region and leads to improved correction results.

The correction of the aerosol scattering effects in the blue spectral region has increasingly caused problems in atmospheric compensation, specifically as new sensors show reasonable radiometric response down to 400 nm wavelength. The traditional atmospheric correction approach is based on an enhanced dark dense vegetation (DDV) approach where aerosol amounts are estimated from dark vegetation signatures, using empirical relations between SWIR spectral bands and the red (650-680 nm) and blue (470-480 nm) spectral region. However, this approach often leads to overcorrections of the deep blue spectral bands (λ < 450 nm) which is visible as a drop-off close to 420 nm (Figure 2). A new approach for a better estimation of aerosol scattering in the blue spectral range has been successfully implemented for space-borne multispectral instruments which enabled the scattering function over dark objects to be extrapolated towards the blue. However, this approach has not led to satisfying results for airborne data yet, because the aerosol signature is weaker and the high spatial resolution often deteriorates the extrapolation. So, there is more research required to improve the atmospheric correction in the blue spectral range.

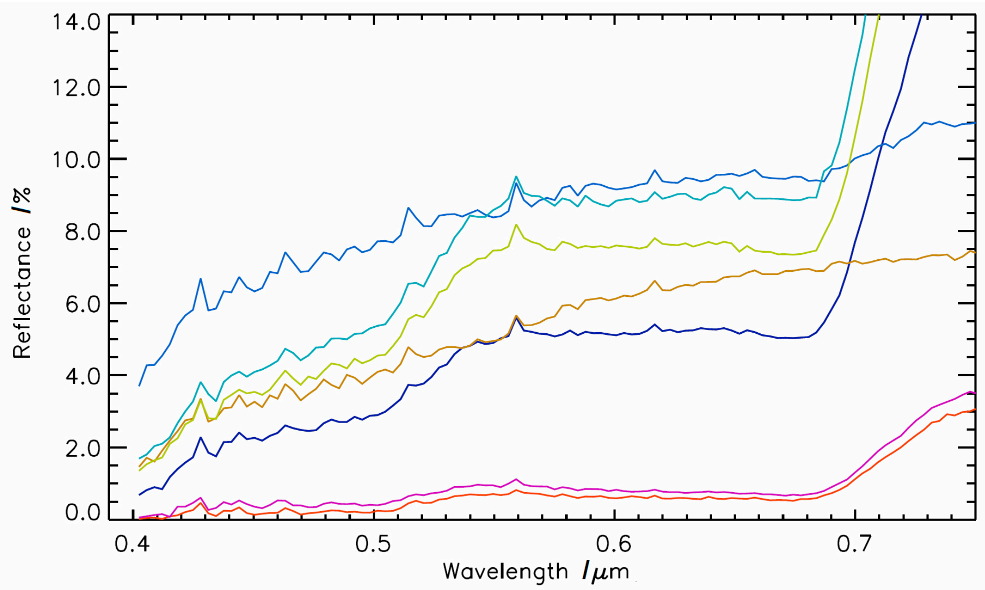

Figure 2: Hyspex1800 sample bottom of atmosphere reflectance spectra of arbitrarily chosen targets in the visible spectral range (25 pixels averaged, 3.2 nm spectral resolution) illustrating drop-off below 420 nm and typical high resolution spectral variations.

BRDF CORRECTION

The BREFCOR (BRdf EFfects CORrection) method has become a part of the ATCOR atmospheric and radiometric compensation process (9). The correction is applied after the atmospheric compensation to convert the *HDRF* to observation-angle independent spectral albedo (*BHR*). The idea is to apply a scaling of the volume scattering and the geometric scattering of the surface cover using the Ross-Thick-Li-Sparse (RTLS) *BRDF* model, which is also used for MODIS data correction (13). A continuous surface characterization index which we call the *BRDF* cover index (*BCI*) is used for this purpose. The index covers all surface types from water to asphalt and concrete, soils, sparse vegetation and dense vegetation as a one-dimensional proxy for *BRDF* types. The *BCI* parameter is formed by an extension of the *NDVI* to non-vegetated surfaces on the one hand and to very densely vegetated surfaces on the other hand.

Before a *BRDF* correction can be applied to the imagery, the RTLS model is calibrated for the various surface types occurring in the imagery by estimating the best fitting kernel weight values.

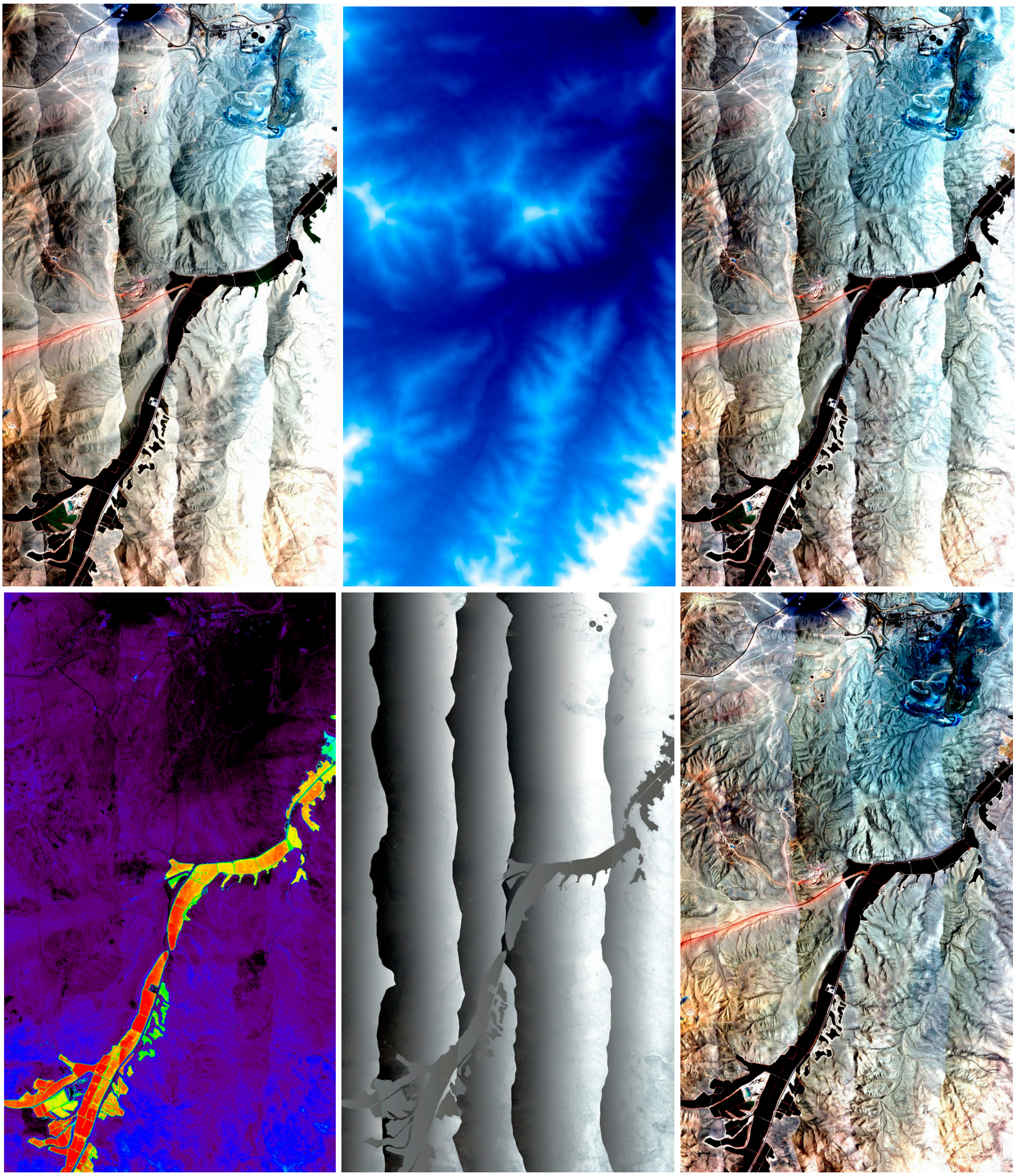

Figure3: Sequence of ATCOR/BREFCOR process for a mosaic of five image lines from Itres CASI-1500. Upper left: original image, middle: elevation data (ranging from 500 to 1,200 m), right: AT-COR standard correction using the given DEM, lower left: BCI image (ranging from -0.5 to 0.8), middle: ANIF factor (ranging from 0.9 to 1.1, approx.), lower right: BREFCOR corrected image.

The BREFCOR correction procedure consists of the following steps:

- perform standard ATCOR atmospheric compensation to bottom of atmosphere *HDRF*
- calculate scene-specific kernels, reduced to the image's solar zenith and relative azimuth angle range
- calculate the *BCI* from image and aggregate in four to seven discrete levels

- calibrate the *BRDF* model for all levels and scenes (i.e., find the geometric and volumetric kernel weighting factors for each of the *BCI* levels), and combine into one generic model
- calculate a spectral anisotropy map by interpolating the kernel weighting factors from the calibrated *BRDF* model using the continuous *BCI* and the observation angles for each image pixel, and
- apply the anisotropy to the imagery on a per-pixel basis.

The final product is a spectral albedo image cube corrected for observation *BRDF* effects. In Figure 3, a sample of this process is illustrated for a CASI-1500 VNIR data set acquired in the Copiapo Mining district in Chile on 17th January 2013. The solar zenith angle was between 13° and 21°, whereas the solar azimuth was at 284° to 299° for the five data strips analysed. The instrument covers the wavelength range from 420 to 1000 nm and uses a FOV of 40°. This large FOV leads to very pronounced across-track *BRDF* effects. The underlying digital elevation model stems from ASTER imagery. ATCOR correction was performed with a 60 km visibility. An overall *BRDF* correction function has been found by a combined analysis of three flight lines. The individual steps of the correction are shown in Figure 3: The top three panels show the ATCOR standard compensation, leaving all BRDF effects untouched but removing the large- scale terrain influence. Based on the *BRDF* model and the *BCI*, the anisotropy can be derived and applied to the *HDRF* data to get a *BHR* output as shown in the last panel.

SPECTRAL ACCURACY

Current imaging spectrometers register spectra at resolutions down to 1 nm in the unbinned mode and an operational resolution of 3-5 nm in the visible spectral range have become very common. Such high spectral resolution puts more demand on both the spectral calibration and the atmospheric compensation routines as shifts of 0.1nm and more are already leading to significant impacts on the spectrum (14). The sample spectra of Figure 2 illustrate this apparently noisy effect in the visible spectral range. In order to keep as much information as possible, extensive spectral polishing is to be avoided and means have to be found to reproduce the physics as closely as possible.

At first, the reference data are to be set correctly, i.e., the solar reference spectrum is to be selected and the most accurate molecular absorption database has to be engaged. The current implementation of ATCOR-4 uses the medium activity solar spectrum as calculated and validated against measurements by Fontenla (10) as a baseline reference. It may be exchanged any time with different solar reference spectra upon availability. Furthermore, the HITRAN 2012 spectral database (15) is used for calculation of the atmospheric transmittance function, using the highest accuracy correlated-k calculations of MODTRAN®5 (16).

Using this foundation, the image-based spectral calibration (11) has been improved by inclusion of Fraunhofer lines and further additional spectral features, such that a total of 15 features are now available for recalibration at the following wavelengths (all in nm): 430, 486, 527, 586, 685, 760, 820, 940, 1,130, 1,268, 1,470, 2,004, 2,055 2,317, and 2,420. The information derived this way may be used for post-calibration of sensor systems from the blue spectral range throughout the SWIR. The smile based processing as described in (11) can then be used for an optimal correction of sharp absorption features from the spectrum.

A further problem which was only taken into account recently is the pressure dependency of the wavelength position of spectral features. All MODTRAN calculations are performed with respect to vacuum frequency and stored as frequency-wave number. Direct translation of the latter into the wavelength domain results in vacuum type wavelength reference data. Most airborne imaging spectrometer systems are operated in unpressurized housings and thus, the registered wavelength is shifted due to the impact of the refractive index of air, which may be well approximated by:

$$n(h) = +0.000293 \cdot e^{-h/H}$$

where H is the scale height (8000 m) and h is the flight altitude. As the effective wavelength is given as

$$\lambda = \frac{c_o f}{n(h)} = \frac{\lambda_o}{n(h)}$$

we can get the effective wavelength on any flight altitude on the basis of the laboratory altitude as:

$$\lambda_{sen} = \frac{\lambda_o}{n(h_{sen})} = \frac{n(h_{lab}) \cdot \lambda_{lab}}{n(h_{sen})},$$

where λ_{lab} is the wavelength measurement performed in the laboratory, and $n(h_{lab})$ is the refractive index of air for the lab height (and corresponding pressure).

The effect of this transition is plotted in Figure 4 for a typical range of flight altitudes. The spectral shift reaches values of up to 0.6 nm at 2,500 nm and up to 0.2 nm in the VNIR spectral range. This effect is even more important in the thermal region, where it can cause shifts of 1 to 3 nm at $\lambda = 10$ µm, depending on flight altitude.

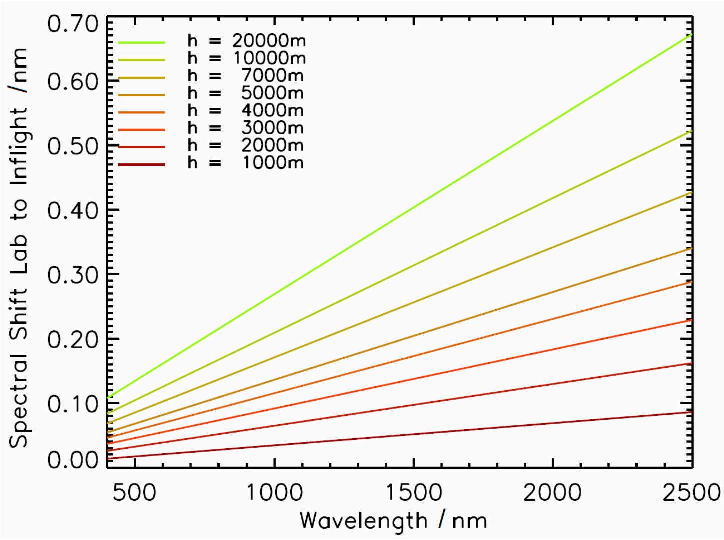

Figure 4: Dependency of spectral shift due to air pressure on flight altitude, assuming a standard laboratory air pressure of 1,013 hPa.

Consideration of this wavelength shift has been included for airborne instruments in ATCOR for VIS/NIR and TIR spectroscopy in a way which takes into account both the laboratory conditions and the sensor pressure configuration. Sensors may be absolutely pressurized or operate at ambient pressure, possibly using some slight overpressure inside the housing. These settings are used when calculating the sensor-specific atmospheric look-up tables (LUT) such that each altitude LUT is derived with a wavelength reference corresponding to the sensor reference. Outputs of atmospheric compensation are finally created at the nominal laboratory reference spectral response.

The impact of this transition is shown in Figure 5 for an average spectrum of a HYSPEX 1800 image scene at a spectral sampling interval of 3.2 nm, in a scene dominated by vegetation. In the reflectance spectra, the difference is only visible within absorption features. The relative difference between wrong pressure assumptions to the real pressure shows the potential error due to pressure differences in a range of 1 to 3% relative error in retrieved reflectance.

More details are visible when checking sample image spectra (Figure 6). The spectral absorptions of oxygen and water vapour may lead to artifacts in the critical red edge range. An improvement can be observed in the spectra when using the correct flight altitude pressure. However, the 760 nm oxygen absorption feature is inconsistently corrected – an effect which cannot be explained by the spectral shift. Such a strong variability of the correction at 760 nm has been observed in similar situations also for CASI and other instruments. This effect can be attributed to an inaccurate description of the spectral band width (*FWHM*). Therefore, the possibility has been introduced in ATCOR to find the best fitting *FWHM* within the characteristic absorption features. The spectral smile aware atmospheric compensation can make use of *FWHM* variations for the processing.

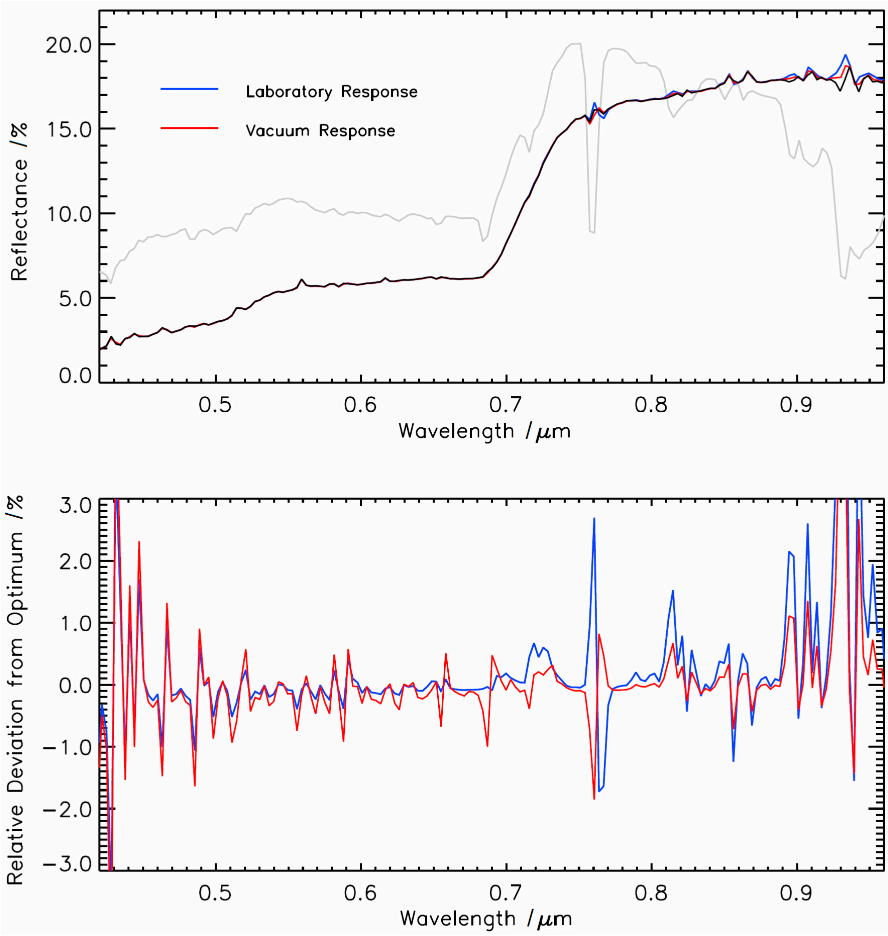

Figure 5: Impact of shifted spectral response due to air pressure on averaged image spectra (one Hyspex 1800 image scene, flown at 3 km a.g.l.). Grey: overlay of radiance spectrum in arbitrary units, black: best spectral position spectrum, blue: laboratory pressure assumption, red: vacuum assumption.

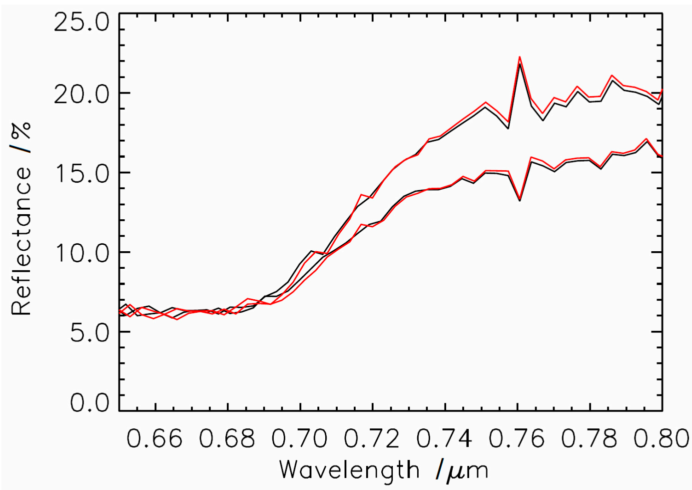

Figure 6: Impact of slight spectral shift on single spectrum appearance in the red edge. Black: optimum position spectrum, red: shifted position at vacuum pressure.

CONCLUSIONS AND OUTLOOK

The development of atmospheric compensation methods is a constantly evolving scientific field and new methods are introduced on a yearly basis. Recently, some issues could be solved: An operational observer *BRDF* correction based on a physical model has been established, a new haze removal method has been developed, improved techniques for spectral calibration have been implemented, and methods for high resolution spectral processing have been established. The ATCOR processing software has come to a state, where fully automatic processing of satellite and airborne imagery is feasible for most standard cases.

For high resolution instruments and demanding terrain situations, however, artifacts appear quite often in both the spectral and spatial domains and methods established for coarse instruments are no longer applicable for operational processing. While some issues have been resolved and new methods have been implemented, there are quite some unresolved problems which remain to be faced.

For the *BRDF* correction, the observer *BRDF* correction has to be coupled with the incidence *BRDF* correction rugged of terrain and spectral auto-correlation should be considered in the future within the chosen model. With an iterative process, the *BRDF* correction will also be capable of solving problems with variations of solar incidence direction and will become truly bi-directional.

A further open issue not mentioned in this paper is the compensation of shadows: for the illumination correction in terrain, a method of consistent and automatic shadow detection and correction remains to be defined. The current implementations are not stable in all situations and therefore not yet well suited for operational use. Also, the description of the diffuse illumination part has to be revisited for that purpose; current tests have shown that methods originally developed for satellite imagery are no longer appropriate for high spatial resolution airborne imaging spectroscopy data. The goal of these developments is to allow for information extraction even from completely shaded areas.

On the spectral accuracy side, combined sensor (re-)calibration of both spectral position and band width is to be envisaged. Secondly, the solar spectrum may have to be revisited, specifically the definitions in the blue spectral range. But, as we work with real data, the polishing routines will surely be required also in the future to make spaceborne or airborne spectral albedo data fit the best to ground reference measurements.

ACKNOWLEDGEMENTS

We acknowledge NEO for providing access to Hyspex1800 imagery and ITRES Research Ltd. is acknowledged for the CASI data set.

REFERENCES

1 Nicodemus F E, J C Richmond, J J Hsia, I W Ginsberg & T Limperis, 1977. Geometrical Considerations and Nomenclature for Reflectance. U.S. Department of Commerce, National Bureau of Standards, 67 pp.

2 Dozier J & J Frew, 1981. Atmospheric corrections to satellite radiometric data over rugged terrain. Remote Sensing of Environment, 11: 191-205

3 Richter R, 1990. A fast atmospheric vorrection algorithm applied to Landsat TM images. International Journal of Remote Sensing, 11: 159-166

4 Thompson D R, B-C Gao, R O Green, D A Roberts, P E Dennison & S R Lundeen, 2015. Atmospheric correction for global mapping spectroscopy: ATREM advances for the HyspIRI preparatory campaign. Remote Sensing of Environment, 167: 64-77

5 Richter R & D Schläpfer, 2015. Atmospheric / Topographic Correction for Airborne Imagery. DLR/ReSe Applications, Wessling, DLR-IB 565-02/15, Version 7.0.1, 252 pp. (last date accessed: 8 January 2016)

6 Lenhard K & A Baumgartner, 2015. Independent laboratory characterization of NEO HySpex imaging spectrometers VNIR-1600 and SWIR-320M-E. IEEE Transactions on Geoscience and Remote Sensing, 53(4): 1828-1841

7 Makarau A, R Richter, R Müller & P Reinartz, 2014. Haze detection and removal in remotely sensed multispectral imagery. IEEE Transactions on Geoscience and Remote Sensing, 52(9): 5895-5905

8 Richter R, T Kellenberger & H Kaufmann, 2009. Comparison of topographic correction methods. Remote Sensing, 1(3): 184-196

9 Schläpfer D, R Richter & T Feingersh, 2015. Operational BRDF effects correction for Wide-Field-of-View Optical Scanners (BREFCOR). IEEE Transactions on Geoscience and Remote Sensing, 53(4): 1855-1864

10 Fontenla J M, J Harder, W Livingston, M Snow & T Woods, 2011. High-resolution solar spectral irradiance from extreme ultraviolet to far infrared. Journal of Geophysical Research, 116(20), D20108

11 Richter R, D Schläpfer & A Müller, 2011. Operational atmospheric correction for imaging spectrometers accounting for the smile effect. IEEE Transactions on Geoscience and Remote Sensing, 49(5): 1772-1780

12 Thompson D R, F C Seidel, B-C Gao, M M Gierach, R O Green, R M Kudela & P Mouroulis, 2015. Optimizing irradiance estimates for coastal and inland water imaging spectroscopy. Geophysical Research Letters, 42(19: 4116-4123

13 Bréon F-M & E Vermote, 2012. Correction of MODIS surface reflectance time series for BRDF effects. Remote Sensing of Environment, 125-C: 1-9

14 Green R, 1998. Spectral calibration requirement for Earth-looking imaging spectrometers in the solar-reflected spectrum. Applied Optics, 37: 683-690

15 Rothman L S, I E Gordon, Y Babikov, A Barbe , D Chris Benner, P F Bernath, M Birk, L Bizzocchi, V Boudon, L R Brown, A Campargue, K Chance, E A Cohen, L H Coudert, V M Devi, B J Drouin, A Fayt, J-M Flaud, R R Gamache, J J Harrison, J-M Hartmann, et al., 2013. The HITRAN2012 molecular spectroscopic database. Journal of Quantitative Spectroscopy & Radiative Transfer, 130: 4-50

16 Berk A, G P Anderson, P K Acharya, L S Bernstein, L Muratov, et al.: MODTRAN5: a reformulated atmospheric band model with auxiliary species and practical multiple scattering options. SPIE Proceedings, 5655, Multispectral and Hyperspectral Remote Sensing Instruments and Applications II, 88, doi:10.1117/12.578758